pH Dependence of Antibody/Lysozyme Complexation†

Cynthia J. Gibas,‡ Shankar Subramaniam,*,‡ J. Andrew McCammon,§ Bradford C. Braden,|| and Roberto J. Poljak||

Department of Molecular and Integrative Physiology, Center for Biophysics and Computational Biology, and National Center for Supercomputing Applications, Beckman Institute for Advanced Science and Technology, University of Illinois at Urbana−Champaign, Urbana, Illinois 61801, Department of Chemistry and Biochemistry, University of California at San Diego, La Jolla, California 92093, and Center for Advanced Research in Biotechnology, University of Maryland Biotechnology Institute, Rockville, Maryland 20850

Received January 28, 1997; Revised Manuscript Received August 19, 1997⊗

ABSTRACT: Association between proteins often depends on the pH and ionic strength conditions of the medium in which it takes place. This is especially true in complexation involving titratable residues at the complex interface. Continuum electrostatics methods were used to calculate the pH-dependent energetics of association of hen egg lysozyme with two closely related monoclonal antibodies raised against it and the association of these antibodies against an avian species variant. A detailed analysis of the energetic contributions reveals that even though the hallmark of association in the two complexes is the presence of conserved charged-residue interactions, the environment of these interactions significantly influences the titration behavior and concomitantly the energetics. The contributing factors include minor structural rearrangements, buried interfacial area, dielectric environment of the key titratable residues, and geometry of the residue dispositions. Modeled structures of several mutant complexes were also studied so as to further delineate the contribution of individual factors to the titration behavior.

In cases where protein association is mediated by charged residues, the energetics of protein association are strongly pH-dependent. Interactions among polar groups at the protein interface often result in large enthalpic contributions to the energetics of association (Buckle et al., 1994). In such cases it is important to assess the ionization states of titratable residues at the protein interface. In this work, we examine two antibody/antigen complexes in which the presence of charge-mediated interactions constitutes a major feature of the protein−protein interface. The two combining regions share several common features; there are salt links and polar group interactions that are the same in each complex. Other components of the electrostatic environment, however, are quite dissimilar in the two complexes. Effects due to desolvation and interactions between polar, noncharged groups are arguably as significant to the electrostatic environment at the interface as charge−charge interactions. In the case of the highly homologous monoclonal antibodies D44.1 and HyHEL-5, which share both a common binding motif in parts of the antigen combining site and a closely related epitope on the surface of hen egg lysozyme (HEL),[1] the affinity of D44.1 for lysozyme is significantly less than that of HyHEL-5, despite the similar charge-mediated interactions in the two antibody/protein interfaces (Sheriff et al., 1987; Benjamin et al., 1992; Tello et al., 1993; Braden et al., 1994; Hibbits et al., 1994, Cohen et al., 1996). The affinity of one antibody (HyHEL-5) for hen egg lysozyme is 3 orders of magnitude greater than that of the other (D44.1). Both HyHEL-5 and D44.1 bind with significantly less affinity to bobwhite quail egg lysozyme (BWQEL), which differs from HEL in only four residues; the only binding site difference is a conservative mutation of Arg68 to a Lys residue. The Arg to Lys mutation does not result in loss of a charge at the interface; more subtle effects of the mutation, including changes in solvation and rearrangements of residues in proximity to Arg 68, appear to contribute to the lower affinity of HyHEL-5 and D44.1 for BWQEL. Four titratable amino acid residues, E35 and E50 in the heavy chain of the antibody (H E35 and H E50), and residues 45 and 68 of the lysozyme (Y R45 and Y R68, or Y K68 in BWQEL), play a key role in association in the D44.1/HEL, HyHEL-5/HEL, and HyHEL-5/BWQEL complexes. Henceforth we use the prefixes H and L to designate the heavy and light chains of the antibody fragment and the prefix Y to designate the lysozyme. Small changes in structure can result in differences in electrostatic potential in the environment of these buried salt links, altering the protonation states of the salt link residues and the pH-dependent behavior of complex formation.

The determination of several structures of antibody/antigen complexes (Amit et al., 1986; Sheriff et al., 1987; Padlan et al., 1989; Bentley et al., 1990; Bhat et al., 1990; Fischmann et al., 1991; Tulip et al., 1992a,b; Chitarra et al., 1993; Prasad et al., 1993; Braden et al., 1994, 1996; Bossart-Whitaker et al., 1995; Chacko et al, 1995, 1996; Bizebard et al., 1995) has made possible an increasingly detailed understanding of the determinants of immune recognition. Site-directed mutagenesis of single residues within the binding interfaces

† This work was supported by National Science Foundation Grant DBI 96-04223 (S.S.), National Institutes of Health Grant R01 GM46535 (S.S.), a metacenter computer allocation (S.S.), National Institutes of Health Grant R01 GM31749 (J.A.M.), and a GAANN graduate research fellowship (C.J.G.)

* To whom correspondence should be addressed.
‡ University of Illinois at Urbana−Champaign.
§ University of California at San Diego.
|| University of Maryland Biotechnology Institute.

⊗ Abstract published in *Advance ACS Abstracts,* December 1, 1997.

[1] Abbreviations: Fv, antibody variable fragment; HEL, hen egg lysozyme; BWQEL, bobwhite quail egg lysozyme; H, antibody heavy-chain fragment; L, antibody light-chain fragment; Y, lysozyme chain; CDR, complementarity determining region; V_L and V_H, variable segments of the light and heavy chains; FDPB, finite difference linearized Poisson−Boltzmann.

S0006-2960(97)00198-0 CCC: $14.00

of antibody/antigen complexes often results in significant changes in binding affinity (Knossow et al., 1984; Alegre et al., 1992; Jin et al., 1992; Chacko et al., 1995). Many recent crystallographic studies of immune recognition have focused on complexes of avian lysozymes with monoclonal antibodies raised against them. (Cohen et al., 1996, Chacko et al., 1995, 1996; Lescar et al., 1996; Braden et al., 1996). Pairs of structures that differ by only a few residues in the binding interface are particularly suited for studying determinants of molecular recognition and complexation.

The association constant for binding of HyHEL-5 to HEL is large (4×10^{10} M^{-1}) (Benjamin et al., 1992); there is a difference of 3 orders of magnitude between it and the association constant for binding of D44.1 to HEL (1.4×10^{7} M^{-1}) (Tello et al., 1993). There is a difference of 2 orders of magnitude between it and the association constant for a lysozyme mutant (Arg68 → Lys) that mimics the epitope of BWQEL (about 1×10^{8} M^{-1}) (Davies & Cohen, 1996; Chacko et al., 1995). However, the combining motifs on the antibody molecules are highly similar, and the recombinant mutant of lysozyme has a single conservative substitution. The binding specificity of antibodies to their antigens involves several factors: surface shape complementarity, electrostatic interactions, hydrogen bonding, hydrophobic packing, and interfacial solvent interactions. Here, we systematically examine and compare the interfacial regions of three antibody/protein complexes of known structure, D44.1/HEL, HyHEL-5/HEL, and HyHEL-5/BWQEL, in order to understand how structural and electrostatic factors may determine differences in antibody/antigen binding. Differences between the D44.1/HEL and HyHEL-5/HEL complexes are substantial enough that all of the above factors may come into play in determining pK_a shifts. Their effects are arguably inseparable, and yet by a detailed examination of the combining regions in these two complexes we can delineate the importance of electrostatic and solvation effects. The comparison of HyHEL-5/HEL and HyHEL-5/BWQEL is more straightforward. A single-residue substitution in the epitope in BWQEL results in changes in electrostatic properties; slight reorganization of the interface creates substantially larger cavities at the interface in the HyHEL-5/BWQEL structure than in HyHEL-5/HEL. A continuum dielectric model and the finite-difference method for electrostatics calculations (Davis et al., 1991; Madura et al., 1995) are used to determine electrostatic potentials and individual amino acid pK_a values in the free antibody, the free lysozyme, and the antibody/lysozyme complex, as well as in several modeled mutant structures.

MATERIALS AND METHODS

Protein Structures. The protein structures used in these calculations are modified versions of coordinates obtained by X-ray crystallography, for the three antibody/lysozyme complexes. These are the complex of the Fab fragment of the mouse monoclonal antibody HyHEL-5 with HEL (Cohen et al., 1996), the complex of the HyHEL-5 Fab fragment with BWQEL (PDB accession code 1BWQEL, Chacko et al., 1996), and the complex of the mouse monoclonal antibody D44.1 with HEL (PDB accession code 1MLC; Braden et al., 1994). The structures are modified to contain only the atoms of the Fv fragment of the antibody, the lysozyme, and buried water molecules located near the antibody/protein interface. Buried water molecules are defined as water molecules less than 20% exposed to bulk solvent; a subset of these are selected in which each water molecule is hydrogen-bonded simultaneously to atoms on the antibody and on lysozyme. This results in three explicit water molecules being left in the antibody/protein interface of the D44.1/HEL complex, four water molecules in the interface of the HyHEL-5/HEL complex, and six water molecules in the interface of the HyHEL-5/BWQEL complex. Because the charge tables used in the pK_a method are parameterized for molecules with polar hydrogen atoms, polar hydrogens are added using the hydrogen positioning program HBUILD (Brunger & Karplus, 1988) within Quanta4.1.[2] A complete study of each native complex requires calculation of pK_a values for four structures: the antibody Fv fragment as excised from the structure of the complex, lysozyme as excised from the complex; the full complex with buried water molecules included, and the full complex without buried water molecules.

Structures of antibody or lysozyme mutants H E35 → Q, H E50 → Q, Y R45 → K, and Y R68 → K are prepared for the D44.1/HEL and HyHEL-5/HEL complexes. In addition, structures for two mutations far from the antibody/protein interface, Y R114 → K and H E46 → Q, are used as controls. These conservative mutations are modeled in the protein structures simply by editing residues and atom names appropriately in the PDB files. A complete study of each mutant complex requires recalculation of pK_a values for two structures: the mutated component (Fv or lysozyme) in isolation and the complex.

Inter- and Intramolecular Interactions. Hydrogen-bonding and nonbonded interactions in the three protein/antibody complexes are analyzed using the program HBPLUS (McDonald & Thornton, 1993).

Calculation of pK_a Values. The method described in Gilson (1993) and Antosiewicz et al. (1994) is used to calculate pK_a values of titrating residues for the antibody/lysozyme complex structures HyHEL-5/HEL, HyHEL-5/BWQEL, and D44.1/HEL and for each of the antibody and lysozyme structures individually. This method implements the UHBD (University of Houston Brownian Dynamics) suite of programs to calculate electrostatic energies (Madura et al., 1995). A modified Tanford−Roxby (1972) approach is then used to determine pK_a values, in which an ionization polynomial is evaluated exactly for clusters of residues with significant charge−charge correlations and a mean field approximation is used for less significant intercluster interactions.

For all calculations, the temperature used is 298 K. A probe radius of 1.4 Å is used to determine the boundary between protein and solvent dielectric, by the method of Shrake and Rupley (1973). A solvent dielectric constant of 80 is used with a protein dielectric constant of 20, except where noted. The cluster method (Gilson, 1993; Antosiewicz et al., 1994) has been found to produce optimal results when a dielectric constant of 20 is used for the protein interior. The ionic strength used in the calculations is 150 mM. FDPB calculations use a finite difference grid of spacing 1.5, and extents 75 Å for lysozyme molecules alone, 90 Å for the Fv fragments, or 120 Å for the full complexes. Smaller focusing grids with spacing 1.2, 0.75, and 0.25 Å and extents 18,

[2] Quanta4.1 is a molecular modeling and display tool developed by Molecular Simulations, Inc. (200 Fifth Ave., Waltham, MA 02254).

```
L- Chain

hyhel5  *26  SSSVNYMYWYQ 36* *45 RWI Y  DTSKLAS 55* *88 QQ    WGRN 93*
              |  |   ||          | |    |   |         ||    | |
d44.1   *26 SQSISNNLHWYR 37* *46 LLIKYVSQSSQSSS 56* *89 QQSN SWPR  96*

H- Chain

hyhel5  *27 YTFSDYWIEW36* *47 WIGEILPGSGSTN*59* * 92GVYYCLHGNYDFDG*105
            |||| |||||        ||||||||||||           ||||  |
d44.1   *27 YTFSTYWIEW36* *47 WIGEILPGSGSTY*59* * 92AVYYCARGDGNYGY*105
```

FIGURE 1: Sequence alignment of CDR and neighboring residues in D44.1 and HyHEL-5. Each of the heavy- and light-chain CDR are labeled. Numbers are sequential starting at N-termini. Gaps have been introduced to maximize homology.

11.25, and 5 Å, respectively, are used to obtain electrostatic potentials in the region surrounding each titrating site. The partial-charge parameters used in the calculation of electrostatic energies are taken from the CHARMm (Brooks et al., 1982) parameter set and radii from the OPLS (Optimized Parameters for Liquid Systems) parameter set (Jorgensen & Tirado-Rives, 1988), following Antosiewicz et al. (1994). Initial pK_a values corresponding to the pK_a values of model compounds in solution for each titrating residue type are taken from Antosiewicz et al. (1994). The cluster method requires that each histidine be assigned a tautomer, i.e., whether the titrating atom in that histidine residue shall be ND1 or NE2. There are three histidine residues in each Fv fragment and a single histidine in each lysozyme molecule. In all cases, the histidine tautomer used is that in which NE2 is the titrating site.

Calculation of Solvent Accessibility and Location of Voids in Protein Structures. The molecular surface of each water-containing structure is calculated using the α shape software developed by Edelsbrunner et al. (1995). α Shape theory provides a method for analytically computing molecular surface areas of proteins. In this method, a simplicial complex called an α-complex is derived from the Delaunay triangulation of the set of atom centers that constitute the protein structure. The Delaunay triangulation is based upon the Voronoi decomposition of the space filled by the protein molecule, in which the space is divided into cells containing one atom each, with each atom "owning" all the space that is closer to that atom than to any other atom. Atoms in the Voronoi diagram correspond to vertices in the Delaunay triangulation, two cells that share a face to a line connecting the vertices, three cells having a common intersection to a triangle connecting the three vertices, etc. The simplicial complex is a complicated object built up from the points, lines, triangles, and tetrahedra of the Delaunay triangulation, and it is combinatorially equivalent to the actual molecule when the radii assigned to each atom center in the Voronoi decomposition are equal to the actual van der Waals radii. Once the α-complex is constructed, algorithms for inclusion and exclusion can be used to exactly determine any metric property of the protein structure (Liang et al., 1996). Differences in solvent-accessible surface area between the complexed and uncomplexed forms of D44.1, HyHEL-5, HEL, and BWQEL are calculated using this method; it is also possible to calculate the contributions of individual residues to the surface of cavities in the protein structure, allowing the visualization of such structures at the protein/antibody interface.

RESULTS

Structural Comparison of Antibody/Protein Pairs. Figure 1 shows the alignment of the D44.1 and HyHEL-5 complementarity determining regions. The antibodies D44.1 and HyHEL-5 differ in only 18 amino acid residues in the Fv region of their heavy (H) chains. Seven of these differences are found to be conservative substitutions of amino acids in the framework of the antibody, while the rest of the differences are found in the complementarity determining regions. There is a single residue difference in the loop extending from H 27 to H 36; residue H 31 is Asp in HyHEL-5 and Thr in D44.1. The second loop, extending from H 47 to H 59 also contains a single difference; residue H59 is Asn in HyHEL-5 and Tyr in D44.1. The remainder of the differences between the two antibody V_H fragments are found between H 92 and H 105; only five residues in this region are conserved (see Figure 1 for the exact sequence). Two conserved residues in the heavy chain, H Glu35 and H Glu50, are directly involved in complex formation. Differences between the light chains of the two antibodies are much more significant. The two light chains differ in 40 amino acid residues. Seventeen of these differences are conservative substitutions of amino acids in the framework (i.e. outside of the antigen binding site); nine are nonconservative substitutions in the framework, and the remainder are substitutions in the CDR. Only 12 residues in the CDR are found to be conserved, and several sequence gaps must be introduced to align these residues.

At the center of the epitope region to which both D44.1 and HyHEL-5 bind on HEL are two residues, Arg45 and Arg68. In BWQEL, Arg68 is replaced with Lys. These two residues protrude from the antibody surface as a ridge in the structures of HEL or BWQEL bound to HyHEL-5; they are hydrogen-bonded to each other. In the structure of HEL bound to D44.1, the side-chain conformation of Arg45 is different and Arg45 and Arg68 are not in as close proximity as in the HyHEL-5 case. The unusual orientation of Arg45 in the D44.1/HEL complex suggests that complex formation is dependent on Arg45 side chain being found in a less-probable orientation in the free HEL (Braden et al., 1994). These residues form three salt links with the two acidic residues in the paratope region of the antibodies, which are found in a cleft in the antibody surface. Residue H Glu35 interacts with Y Arg68; this interaction is direct in the D44.1 case and mediated by water in the HyHEL-5 cases. Residue H Glu50 interacts with both Y Arg45 and Y Arg68.

Despite the essential similarity of these salt link interactions in the D44.1/HEL and HyHEL-5/HEL complexes, the mode of binding of the two antibodies to HEL is significantly

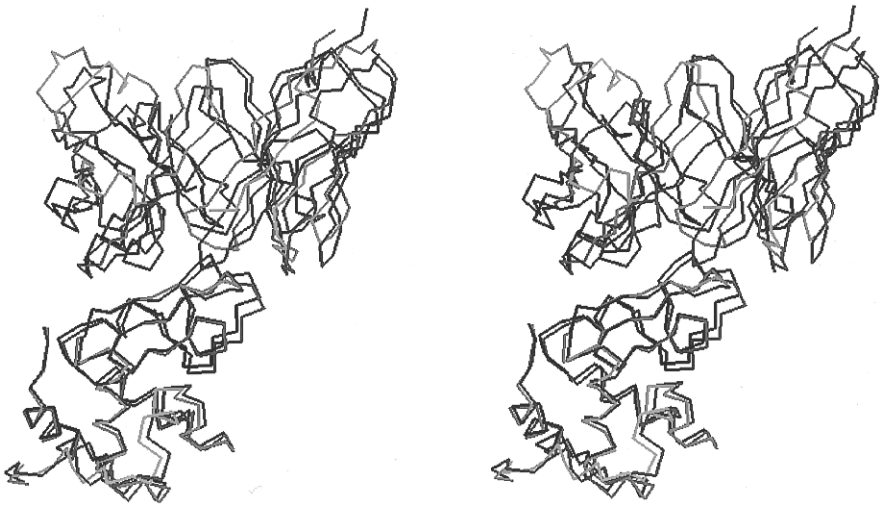

FIGURE 2: Stereo view of superimposed structures of the D44.1/HEL complex and the HyHEL-5/HEL complex. The HEL chains have been aligned to show the relative positions of the antibody in each complex. The D44.1/HEL complex is shown in light gray; the HyHEL-5 complex is in darker gray.

FIGURE 3: Stereo view of superimposed structures of the D44.1/HEL complex and the HyHEL-5/HEL complex. The H chains of each antibody have been aligned to show the different geometry of the L chain with respect to the H chain. Display conventions are the same as in Figure 2.

different, as shown in Figure 2. This figure shows the structures of the two antibody/lysozyme complexes superimposed, with the lysozyme chains aligned. Using this frame of reference, the two bound antibodies are offset from one another, with a distance of 1−3 Å between corresponding α carbons in the two antibody structures. The RMS difference between the two complexes, for all equivalent atoms, is 2.48 Å. When the lysozymes are aligned, single-residue RMS differences are as large as 12.0 Å in the antibody Fv fragment, but RMS differences range from 0.1 to 5 Å in the lysozyme. While the offset between the two structures means that residues distant from the combining site have the largest RMS values, there are local maxima in RMS difference in the altered CDR regions. Not only does the position of the antibody with respect to the lysozyme differ in the D44.1/HEL and HyHEL-5/HEL structures, but the orientation of the two antibody chains with respect to each other differs as well; Figure 3 shows the antibody/lysozyme complex structures with the H chain superimposed. The mode of binding of HyHEL-5 to HEL and BWQEL, on the other hand, is nearly identical; when the two lysozyme structures are superimposed in this case, HyHEL-5 bound to HEL is not offset with respect to HyHEL-5 bound to BWQEL. The RMS difference between the two structures, for all equivalent atoms, is 0.58 Å; on a per-residue basis, RMS difference between equivalent atoms varies between about 0.15 and 1.5 Å. Some of the largest single-residue differences are found in the antibody paratope region, affecting residues L 31, L 50, H 35, and H103 among others, while the epitope, including residue 68, is largely unperturbed by the single-residue difference.

Table 1 summarizes the $C_\alpha-C_\alpha$ distances between V_L and V_H residues in the antibody framework, which are characteristic of mouse antibodies with κ L chains, comparing the average distance with the distances in these antibody/lysozyme complexes. While most of these framework V_L-V_H contacts are conserved in both D44.1 and HyHEL-5, there are two regions in that the contacts differ in the two antibodies. The loop region which contains residues 92−95 is longer, in D44.1, by one residue; an insertion of three residues prior to L Trp90 (relative to HyHEL-5) displaces the Trp to position L 94 and L Arg92 to position L 96. The contact between L 94 and H 47 is substantially different in D44.1 because of the lengthening of this loop. The displacement of the Trp residue and resulting structural changes have significant implications for electrostatics. Table 2 sum-

Table 1: $C_\alpha - C_\alpha$ Distances between Residues in the L and H Domains of Mouse Antibodies with κ Chains

residues	average all κ (Å)	distance in D44.1/HEL cplx (Å)	distance in HyHEL-5/HEL cplx (Å)
L 36−H 103	10.97 ± 0.36	11.41	11.11
L 43−H 91	8.19 ± 0.59	7.72	7.67
L 43−H 103	6.69 ± 0.54	6.58	6.80
L 44−H 45	9.80 ± 0.65	9.85	9.82
L 44−H 91	9.56 ± 0.31	9.61	8.99
L 44−H 103	6.98 ± 0.44	7.39	7.20
L 46−H 101	5.17 ± 0.75	5.42	7.22
L 87−H 45	8.65 ± 0.39	8.78	8.53
L 94−H 47	9.69 ± 0.60	8.89	7.98
L 94−H 58	8.89 ± 1.19	9.22	8.80
L 95−H 47	7.23 ± 0.42	6.26	6.07
L 96−H 47	6.37 ± 0.28	6.12	6.36

Table 2: Geometry of Charged Residue Interactions in the Three Antibody/Lysozyme Complexes

atom 1	atom 2	D−A distance (Å)	D−H−A angle (deg)
		D44.1/HEL	
H 35 OE	Y 68 NH	2.93	171.7
H 50 OE	Y 68 NH	2.51	122.9
H 50 OE	Y 45 NH	3.03	134.4
		HyHEL-5/HEL	
H 50 OE	Y 45 NH	2.97	148.2
H 50 OE	Y 68 NH	3.30	137.3
H 35 OE	O(H_2O)	2.76	143.7
O(H_2O)	Y 68 NH	2.84	138.0
		HyHEL-5/BWQEL	
H 50 OE	Y 45 NH	2.92	159.3
H 50 OE	Y 68 NZ	3.56	137.4
H 35 OE	O(H_2O)	2.91	173.3
O(H_2O)	Y 68 NZ	3.78	136.6

marizes the resulting changes in the geometry of the crucial salt links at the antibody/lysozyme interface; in D44.1 bound to HEL these distances are short and the interactions between the basic residues on the surface of the lysozyme and the acidic residues in the cleft of the antibody are direct. In HyHEL-5 bound to HEL the distances are longer and the salt-link interactions are mediated by water molecules.

The interface region of HEL bound to D44.1 is smaller, with 1248 Å^2 of protein surface buried, and less complex than the interface of HEL bound to HyHEL-5, in which 1510 Å^2 of protein surface is buried. Though there is only a single-residue difference at the interface in BWQEL, BWQEL bound to HyHEL-5 has an even larger interface, in which 1600 Å^2 of protein surface are buried. The salt-link residues Arg Y45 and Y Arg68 are separated at the D44.1/HEL interface due to a rotation of the side chain of Y Arg45; in the HyHEL-5/HEL complex they are in close contact, and Y Arg45 penetrates more deeply into HyHEL-5 than into D44.1. Y Arg61 forms part of the interface when either HEL or BWQEL bind to HyHEL-5, while it is rotated far out of the interface region when HEL binds to D44.1. On the other side of the interface, L Arg96, which is in a central position of the paratope region of D44.1, is not present in HyHEL-5. Instead, Arg L92 is found at the edge of the paratope region. Residues L Asp49 and L Asp31 play a role in the interface region of HyHEL-5 with both avian lysozymes; these residues have no counterpart in the interface of D44.1 with HEL. Figure 4 shows a view of the antibody/lysozyme interface in which hydrogen bonds are drawn explicitly between the various residues. In this view it is possible to

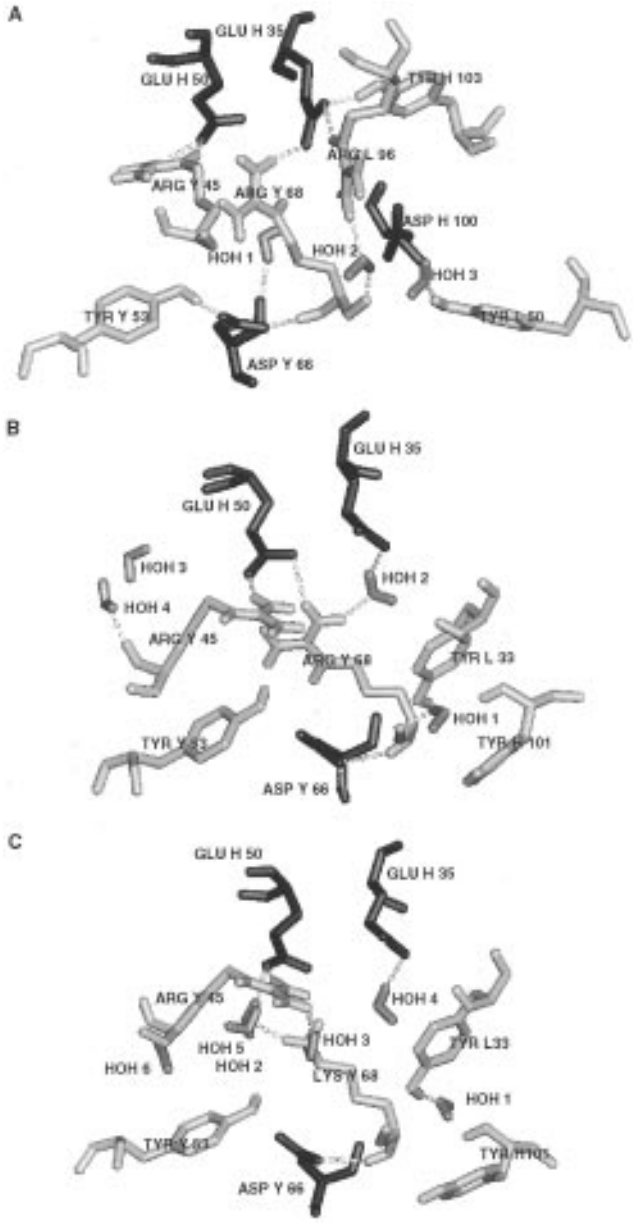

FIGURE 4: Salt link residues and their interactions in (A) D44.1/HEL, (B) HyHEL-5/HEL, and (C) HyHEL-5/BWQEL. Water molecule hydrogen positions were calculated using HBUILD (Brunger & Karplus, 1988).

see that L Arg96 participates in the salt link interactions between D44.1 and HEL, forming an intra-Fv link with H Glu35 (Figure 4A) while its counterpart L Arg92 in HyHEL-5 does not (Figure 4B,C). The position of L Arg96 is in part determined by the position of the Trp side chain at L 94, which forces it to assume an unusual conformation in D44.1. L Asn92 forms a hydrogen bond with Thr 47 of HEL, a hydrogen bond between L Trp94 and H Glu50 is broken, and the loop including residues L Ser93−L Arg96 shows a concerted movement away from HEL apparently due to the orientation of Arg45 of HEL (Braden et al., 1994).

Residues that make up a significant part of the buried surface in HyHEL-5 and not in D44.1 include L Asn30, which is replaced by Ser in D44.1; L Tyr31, which is replaced by Asn in D44.1; L Trp90, which is replaced by Gln in D44.1; and H Tyr101, which is replaced by Gly in D44.1. The salt-link residues H Glu35 and H Glu50 are more than 80% inaccessible to solvent in both the free

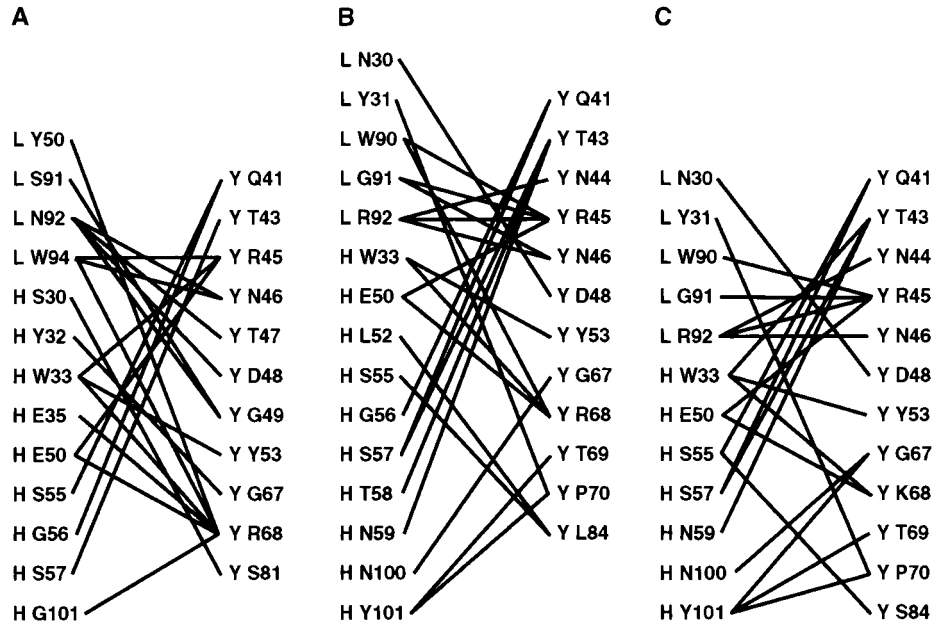

FIGURE 5: Contact maps of the antibody/lysozyme interface for (A) D44.1/HEL, (B) HyHEL-5/HEL, and (C) HyHEL-5/BWQEL. Contacts are indicated for residues on opposite sides of the interface only and do not include contacts with water molecules; the cutoff distance used is 3.6 Å. Contacts shown were obtained using the program HBPLUS (McDonald & Thornton, 1993).

antibody structures and therefore undergo little change in solvent accessibility upon antibody binding to lysozyme. Figure 5 shows the nonpolar contacts between residues at the antibody/protein interface in each of the three complexes. The pattern of contacts between HyHEL-5 and BWQEL differs very little from the pattern of contacts between HyHEL-5 and HEL; even between D44.1 and HEL the majority of the nonpolar contacts are very similar to those between HEL and HyHEL-5. A number of residues, including H Asn100, H Asn59, H Thr58, and H Leu52, that contact HEL in HyHEL-5 are absent at the D44.1 interface. This reflects the smaller area of the paratope region in D44.1 and in that sense is significant for binding, as buried interface area is an important determinant of affinity (Janin, 1995). It is also significant in defining the local dielectric environment around the charge pair residues.

In Figure 6, the three protein/antibody complexes are shown in wire-frame representation, in similar orientations, with cavities in their structures shown as polyhedra. The lobe at the lower left of each structure is the lysozyme molecule, while the lobe at the upper right is the antibody heavy chain and the lobe at the lower right is the antibody light chain. Also shown in Figure 6 are ribbon diagrams of the complexes, showing the location of buried water molecules at the antibody/protein interface. There are three water molecules in D44.1/HEL, four in HyHEL-5/HEL, and six in HyHEL-5/BWQEL. The larger cavity space available for water molecules in the latter two structures is reflected in the number of void polyhedra present at the interface between antibody and lysozyme in each of the structures. In the HyHEL-5/HEL and HyHEL-5/BWQEL complexes, the size and number of void polyhedra in the area of the interface is much greater, and this is reflected in the number of water molecules that are bound at these interfaces. It has been suggested (Bhat et al., 1994; Braden et al., 1995; Goldbaum et al., 1996) that water molecules may actually mediate antibody/protein interactions to some extent, rather than merely being spectator molecules in the interface. The single-residue substitution in BWQEL makes a difference in the number of water molecules that are found buried at the antibody/lysozyme interface; only four water molecules are found in the HyHEL-5/HEL complex, and six in the HyHEL-5/BWQEL complex.

Figure 7 shows schematic diagrams of hydrogen bonding across the antibody/protein interface. Twenty hydrogen bonds bridge the interface between D44.1 and HEL, of which only eight are direct contacts between protein and antibody. The remainder of the hydrogen bonds involve one of the three water molecules bound at the antibody/protein interface. There are 25 hydrogen bonds bridging the HyHEL-5/HEL interface, of which 14 are directly between antibody and protein atoms, and 23 in the HyHEL-5/BWQEL interface, of which seven are directly between antibody and protein atoms. The larger cavities at the interface in the HyHEL-5/BWQEL complex result in solvent-mediated hydrogen bonding between the antibody and the epitope. In both D44.1/HEL and HyHEL-5/HEL, H Glu35 is hydrogen-bonded to Y Arg68. In the HyHEL-5/HEL complex, however, this interaction is mediated by one of the water molecules bound at the antibody/protein interface. In HyHEL-5/BWQEL, there is no hydrogen bond between H Glu35 and Y Arg68. Instead, H Glu35 is hydrogen-bonded only to one of the water molecules at the interface, and Y Lys68 is hydrogen-bonded to H Glu50 through another of the water molecules. In all three complexes, H Glu50 is directly hydrogen-bonded to Y Arg45. Other residues that form hydrogen bonds to the salt-link residues in D44.1 are L Tyr50 (to Y Arg45) and L Arg96 (to Y Arg68, through one of the interfacial water molecules). Neither of these interactions has an exact counterpart in the HyHEL-5 complexes, though L Arg92 is hydrogen-bonded to Y Arg45 in those cases, as is L Trp90 in the HyHEL-5/HEL complex.

Electrostatic Effects. Figure 8 shows the complementary molecular surfaces of each antibody/antigen pair. The green circles highlight the salt-link residues on each protein surface, where the two basic residues appear as a blue protrusion on the surface of the lysozyme (Figure 8B,D,F) and the acidic residues appear as a region of large negative potential within

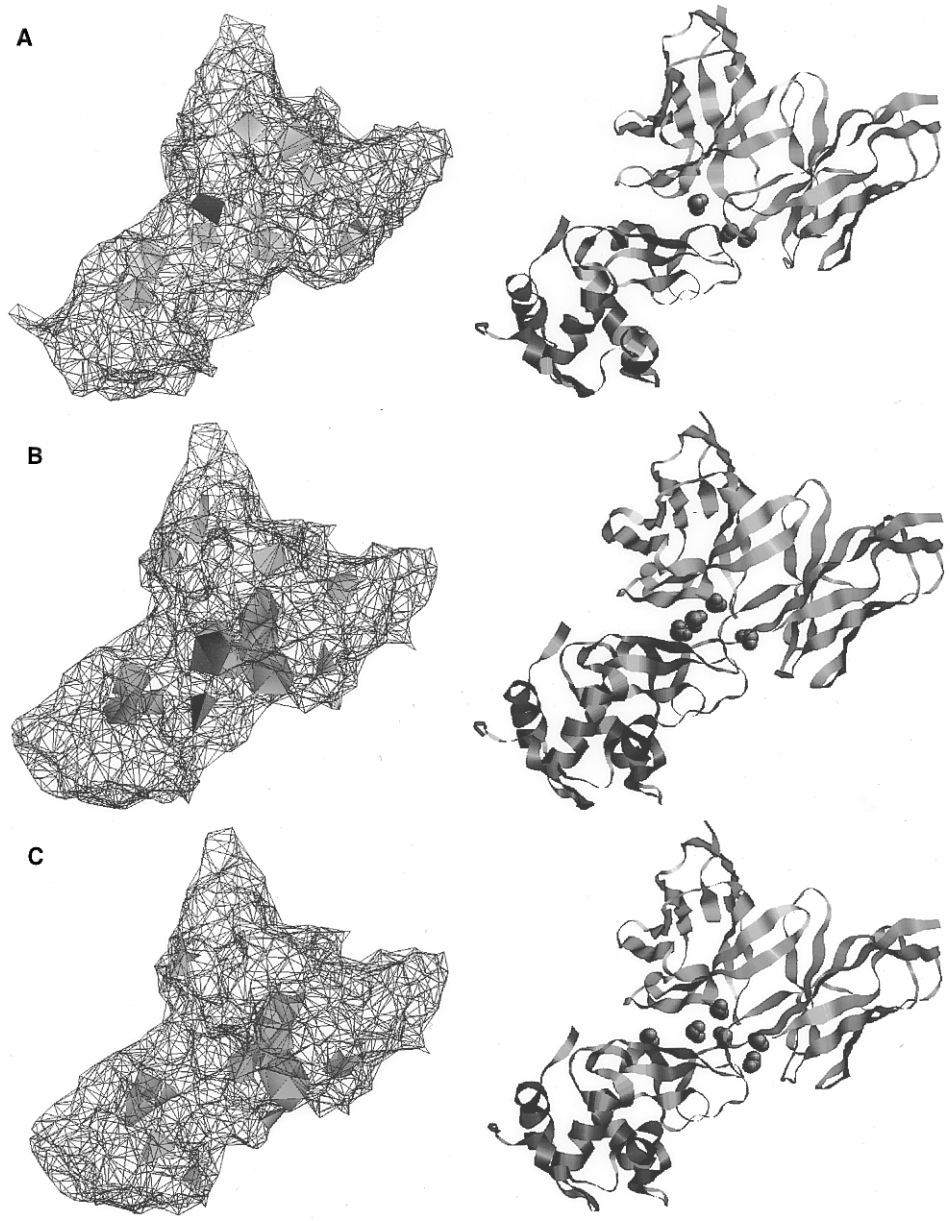

FIGURE 6: Voids in the protein complexes, calculated using VOLBL, and locations of buried solvent molecules at the interface. The complexes are shown in wire-frame representations with voids, shown as shaded solid polyhedra, on the left and in ribbon representation, with the locations of buried waters, shown as spheres, on the right. (A) D44.1/HEL; (B) HyHEL-5/HEL; (C) HyHEL-5/BWQEL.

a hole on the surface of the antibody (Figure 8A,C,E). The shape complementarity between the two halves of each complex, especially between the ridge formed by the basic residues on the lysozyme surface and the groove in which the acidic residues lie on the antibody, is obvious even though voids are known to be present at the interfaces. The visible differences in potential that may contribute to differences in association constants of the three complexes include the larger positive potential at the basic residues of HEL and BWQEL as bound to HyHEL-5. In HEL as bound to HyHEL-5, Y Arg45 assumes a slightly different conformation than in HEL as bound to D44.1. In the HyHEL-5/HEL structure, the charged groups of the two arginine residues Y 45 and Y 68 are somewhat closer together, though by less than 0.5 Å, than in the D44.1/HEL structure; the same is true for the arginine and lysine residues Y 45 and Y 68 in the HyHEL-5/BWQEL structure. Visible differences in the antibody surface potential include a small region of positive potential near the salt-link residues, probably due to the location of L Arg96 at the interface, which has no counterpart in HyHEL-5, and the large negative potential at peripheral points surrounding the binding site of HyHEL-5, perhaps due to the presence of two Asp residues near the interface which have no counterpart in D44.1.

Electrostatic contacts between antibody and antigen in the three antibody/lysozyme complexes are summarized in Figure 9. These are the site−site interaction energies W_{ij} obtained in the pK_a calculation. The interaction energy in kilocalories per mole is a measure of the effect that each individual residue will have on the pK_a values of other individual residues; the combined effects of all residues with nonzero interaction energy with a particular titrating site result in the total pK_a shift to that site. Therefore, the pattern of nonzero interaction energies is a means of finding electrostatic interactions between titrating sites in the protein. Multiple interactions between a number of titrating sites influence the apparent pK_a value of any particular residue in a complex fashion, but the interactions W_{ij} are a measure

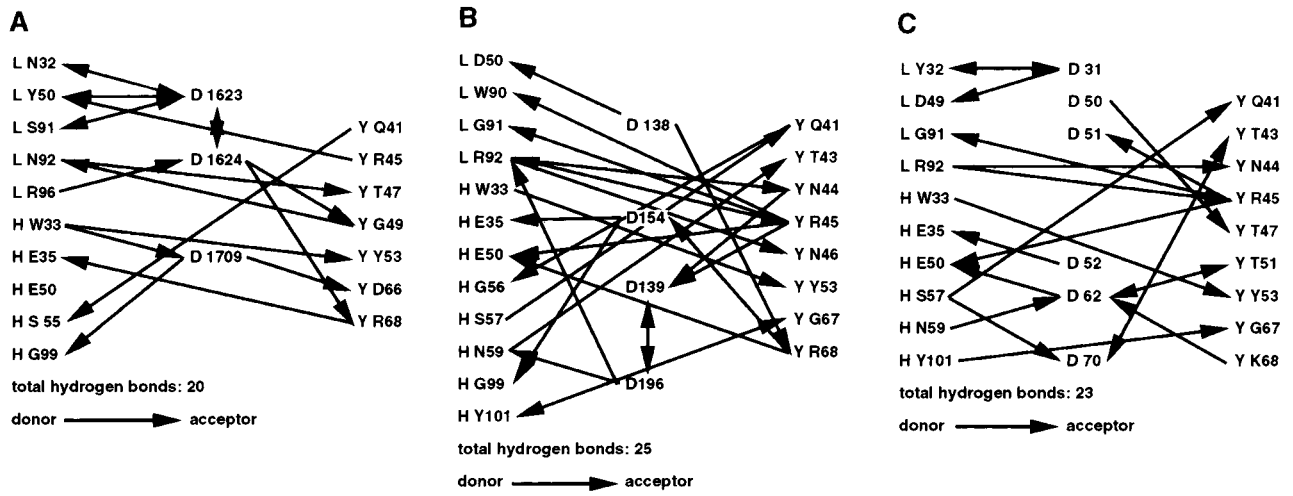

FIGURE 7: Hydrogen-bonding map of the antibody/lysozyme interface for (A) D44.1/HEL, (B) HyHEL-5/HEL, and (C) HyHEL-5/BWQEL. Hydrogen bonds are indicated for residues on opposite sides of the interface, or between water molecules and residues on either side of the interface, only. Unidirectional arrows indicate by direction the donor and acceptor in the H-bond as shown. Bidirectional arrows between a pair of residues indicate two or more hydrogen bonds between those residues. Hydrogen bonds were obtained using HBPLUS (McDonald & Thornton, 1993).

of the influence individual residues have on each other. In general, many of the interactions between particular residues in the three complexes remain the same, changing only by 0.1−0.2 kcal/mol. Larger changes suggest that the change in a particular interaction may have an effect on association. The interactions between the basic residues Y 45 and Y 68 of the lysozymes and the acidic residues H Glu35 and H Glu60 differ little between the HyHEL-5/HEL complex and the HyHEL-5/BWQEL complex and much more significantly between the HyHEL-5/HEL complex and the D44.1/HEL complex. But to begin to account for the large differences in binding between the two complexes, it is useful to note the presence of residues that have strong interactions with the salt-link residues in one complex and negligible interactions in the others; for instance, L His34, L Arg96, and H Asp100 of D44.1 and L Tyr33, L Tyr35, and H His98 of HyHEL-5.

pH-Dependent Behavior of Wild-Type Antibody−Lysozyme Complexes. Calculated changes in free energy on binding are shown in Figure 10 over the pH range 0−14. At pH 7.0, the change in free energy on complex formation is negative for each of the antibody/lysozyme pairs. The calculated ΔG_{elec} of binding for the HyHEL-5/HEL pair is −4.4 kcal/mol; there is a difference of +1.2 kcal/mol between the changes in free energy on binding for the D44.1/HEL complex and the HyHEL-5 complex and a difference of +1.4 kcal/mol for the HyHEL-5/BWQEL complex and the HyHEL-5 complex. Though the purely electrostatic change in free energy calculated here cannot be expected to fully account for the strength of antibody/protein association observed in these three complexes, the relative changes in free energy among the three complexes are of the correct sign and of reasonable magnitude. At the low extreme of the pH range, H Glu35 and H Glu50 become protonated. Complex formation then involves the burial of two positively charged Arg residues at the interface where no corresponding negative charges are present, and the calculated change in free energy on binding is large and positive. At the high extreme of the pH range, Arg45 and Arg68 of the lysozyme become deprotonated; however, as the residues H Glu35 and H Glu50 are not solvent-exposed in the uncomplexed antibody structure, the burying of these charges in an environment where no compensating charges exist is not a large component of the free energy change on binding. The minimum free energy change on binding for each of the antibody/lysozyme complexes occurs around pH 13.

Individual Residue Protonation States and pK_a Values. The D44.1/HEL complex has 87 titrating sites, a largest possible positive charge of +41.0, and a largest possible negative charge of −46.0; the HyHEL-5/lysozyme complexes both have 88 titrating sites, a largest possible positive charge of +41.0, and a largest possible negative charge of −47.0. At pH 7, the total charge on the D44.1/HEL complex is 6.1, while the total charge on the HyHEL-5/complex is 6.4 and the total charge on the HyHEL-5/BWQEL complex is 7.1, a difference of only 0.3 proton between the two antibody complexes with HEL but a difference of 0.7 proton between the two HyHEL-5 complexes. This difference in protonation, however, is distributed over the protein, rather than localized to a particular residue. The changes in fractional protonation calculated by McDonald et al. (1995) were not seen in this study. This may be due to the different structure models of the HyHEL-5 complex that were used in the two studies, as well as to choice of different grid parameters in calculation of electrostatic interaction energies and use of a dielectric of 20 here, rather than 4, to represent the protein interior. We have found in previous computational studies (Gibas & Subramaniam, 1995) that while calculated pK_a values are sensitive to the choice of dielectric constant, this sensitivity may be mitigated by the choice of appropriate parameters in the electrostatics calculations.

Figure 11 summarizes significant pK_a shifts due to complex formation in the three antibody/lysozyme complexes. These data are shown in the context of all of the titrating sites in the protein; it can be seen that pK_a shifts are well-localized to particular residues at the antibody/protein interface, while outside those regions pK_a shifts are negligible. While by far the largest pK_a shifts are those to Y Arg or Lys 68, and to the other salt-link-forming residues, there are a number of other residues near the interface that are affected. The pK_a values of the acidic residues H 35 and H 50 are shifted in a negative direction relative to their pK_a values in the free antibodies, though the pK_a of H Glu35, which is almost completely inaccessible to solvent even in

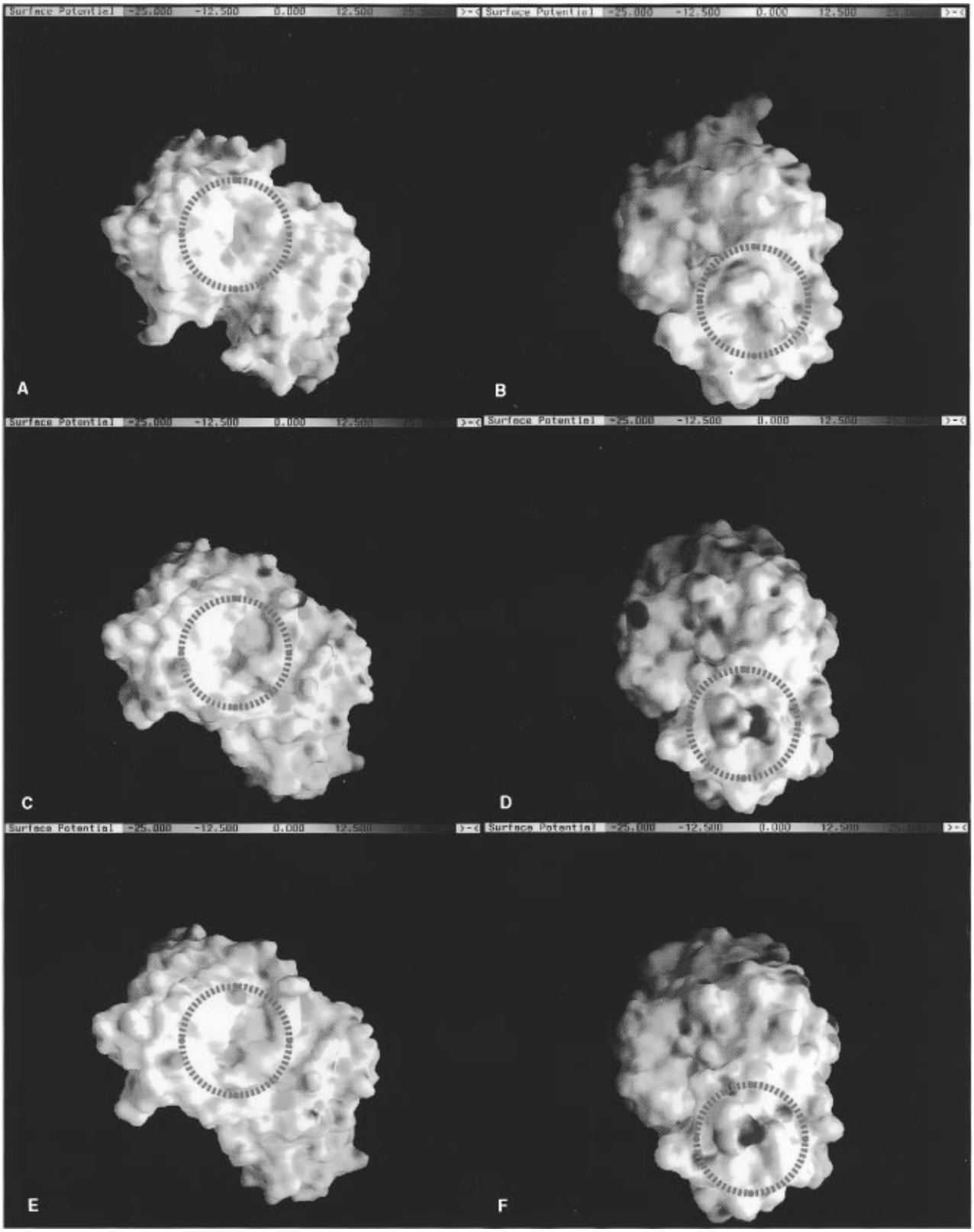

FIGURE 8: Complementary surfaces of lysozyme and antibody molecules. Molecular surfaces are colored according to the electrostatic potential interpolated to individual atoms in the free lysozyme and antibody. Salt-bridge residues are located within the green circles. (A) Surface of D44.1 that contacts HEL. The protrusion on the surface of HEL, which is due to arginine residues 45 and 68, can be seen to fit into the corresponding concavity on the surface of D44.1, if the molecule is rotated 180° around the vertical axis and superimposed on D44.1. (B) Surface of HEL as it binds to D44.1. (C) Surface of HyHEL-5 as it binds to HEL. (D) Surface of HEL as it binds to HyHEL-5. Increased positive potential near the arginine residues, with respect to view A, is due to conformational changes which bring them into closer proximity to each other. (E) Surface of HyHEL-5 as it binds to BWQEL. Panels A−E were generated using GRASP. (F) Surface of BWQEL as it binds to HyHEL-5 (Nicholls et al., 1991).

the free antibodies, undergoes a rather small shift, implying that preexisting interactions with that residue within the antibody molecule may stabilize it in its preferred ionization state. These include intramolecular hydrogen bonding to L Arg96 in D44.1, the side chain of which is forced into proximity with H Glu35 due to the unusual sequence of light

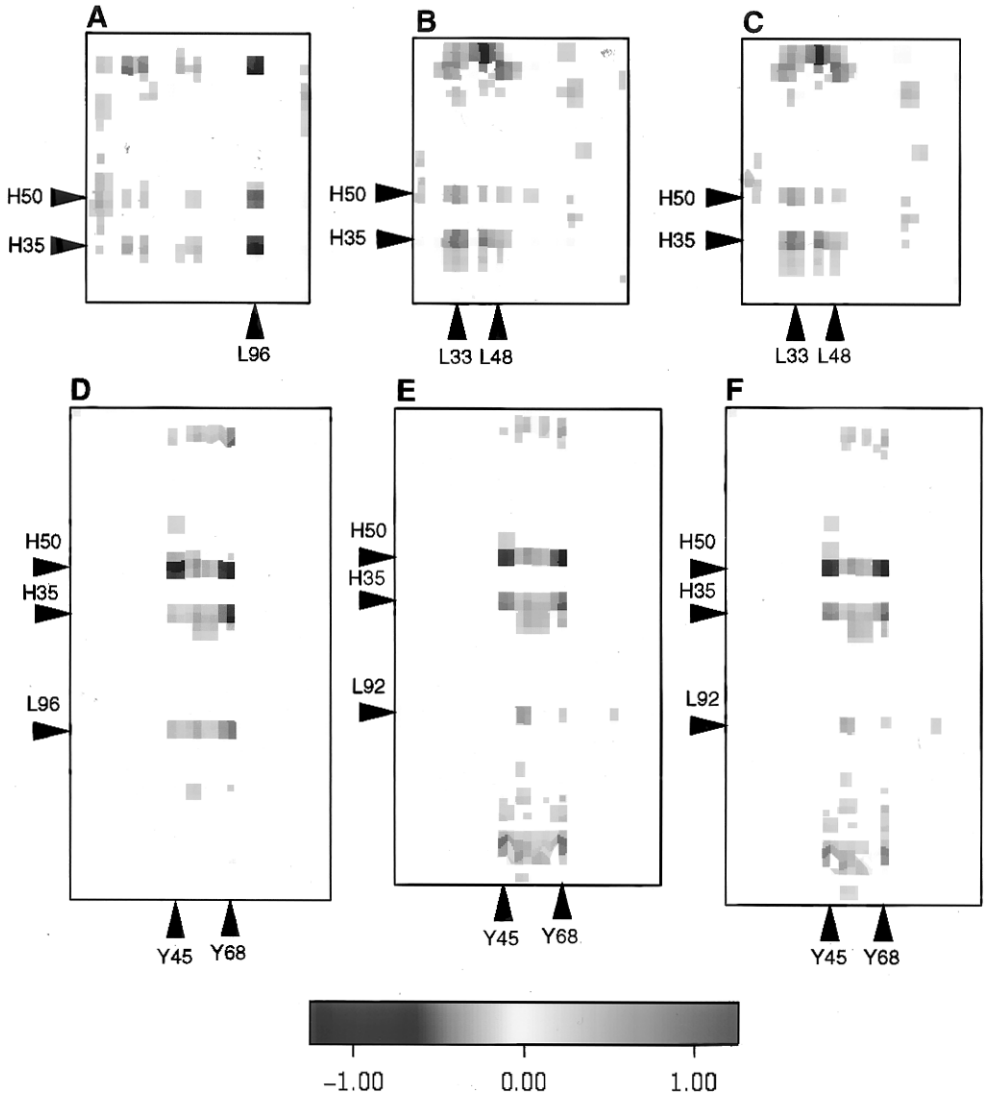

FIGURE 9: Electrostatic interaction maps. The value plotted is the interaction energy W_{ij} for each pair of titrating sites, in kilocalories per mole. Favorable interactions are shown in blue and unfavorable interactions in red. Positions in the sequence of residues of interest are indicated. (A−C) interactions between residues in the L (*x*-axis) and H (*y*-axis) chains. (D−F) Interactions between residues in the lysozyme (*x*-axis) and antibody (*y*-axis).

chain CDR 3, which has Trp at position L 94 instead of the more common Ser. The pK_a values of the basic residues Y 45 and Y 68 are shifted in a positive direction relative to their pK_a values in the free lysozyme molecules. The result in each case is that the ionization equilibrium of each residue is shifted toward the charged form, indicating that two ion pairs exist at the antibody/protein interface in each of the three protein complexes. The titration curves of the individual salt-link residues show no unusual titration behavior; all of these residues have classical titration curves in the free antibody and lysozyme that are only slightly altered in shape between the complexes (Figure 12). The effect of increasing ionic strength on these residues is predictable and relatively insignificant compared to the differences in their titration behavior among the three antibody/protein complexes. Significant shifts that imply participation of particular residues in binding are those to L Tyr33 and H Tyr101 of HyHEL-5, L Arg96 of D44.1, and Y Tyr53 of both lysozymes. Of these residues, only H Tyr101 of HyHEL-5 actually undergoes a significant change in solvent accessibility on binding. The rest of the residues are found within 5 Å of the combining site and are mostly solvent-inaccessible in the free protein.

Table 3 summarizes residues that change protonation states on binding at pH 7.0. Results of calculations using a protein interior dielectric constant, ϵ, of 20 are shown in section A, while results of calculations using $\epsilon = 4$ are shown in section B. While no significant changes in protonation are calculated when $\epsilon = 20$, H Glu50 is found to go from nearly 100% protonated in the free antibody to 100% ionized in the complex when $\epsilon = 4$. This is similar to the results obtained by McDonald et al. (1995). However, use of a protein interior dielectric constant of 4 to represent the whole protein often results in overshifted pK_a values, and using an internal dielectric constant of 20 better represents the dielectric environment in the interface between antibody and protein (Gibas & Subramaniam, 1996). The presence of several charged residues in the interface creates a polarizing environment, and there are a number of water molecules in the antibody/protein interface in each of the crystal structures used. Both conditions suggest that a dielectric constant higher than 4 is appropriate.

Inclusion of Selected Water Molecules. Previously, we have found that inclusion of selected water molecules explicitly in the protein structures used for continuum electrostatics-based pK_a calculations may improve results in

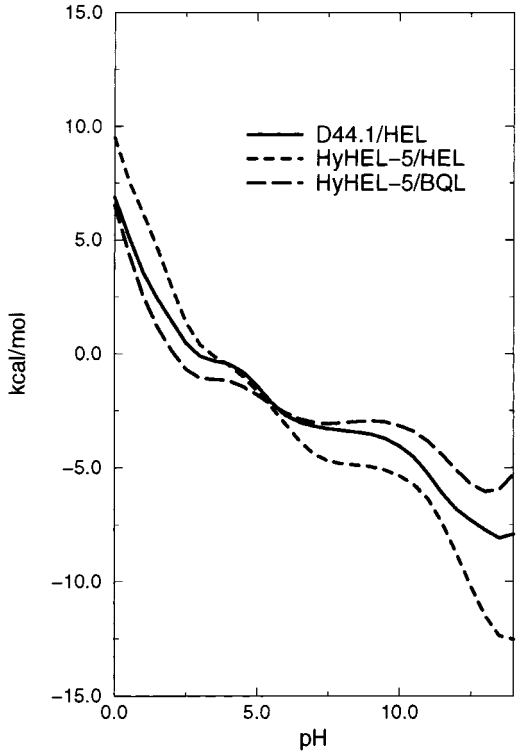

FIGURE 10: Change in free energy on binding [$G_{elec,complex} - (G_{elec,antibody} + G_{elec,protein})$] vs pH for the three antibody/protein complexes.

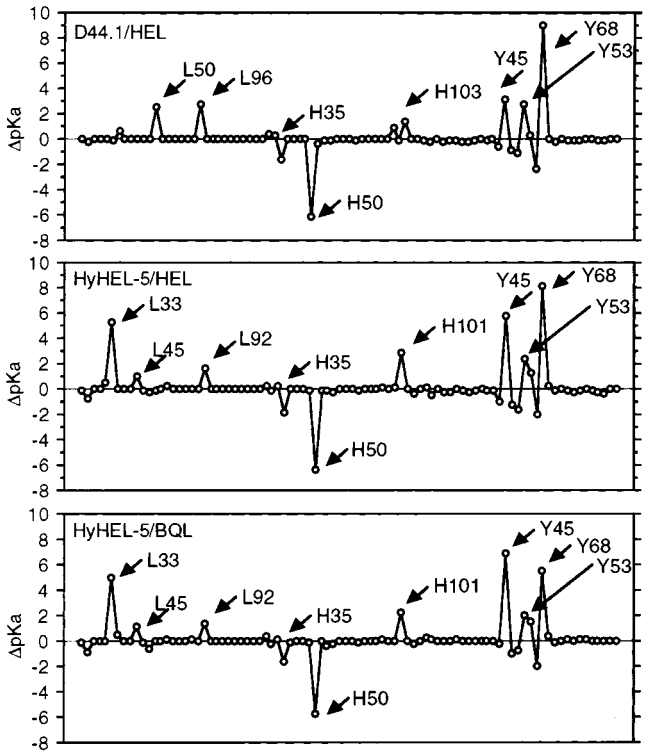

FIGURE 11: Calculated pK_a shifts on binding in each of the three antibody/lysozyme complexes, vs residue number.

some cases (Gibas & Subramaniam, 1996). In this calculation, we chose to include only water molecules bound near the antibody/protein interface, so that 3−6 water molecules/protein complex were included. Outside this region of interest a standard continuum model was used. Table 4 summarizes the effects of adding these water molecules to the protein structure; the largest pK_a shift due to the placement of a water molecule near a residue was 0.9 pH unit. Any effect of inclusion of the explicit water molecules, however, was negligible compared to the pK_a shifts that occur upon complex formation.

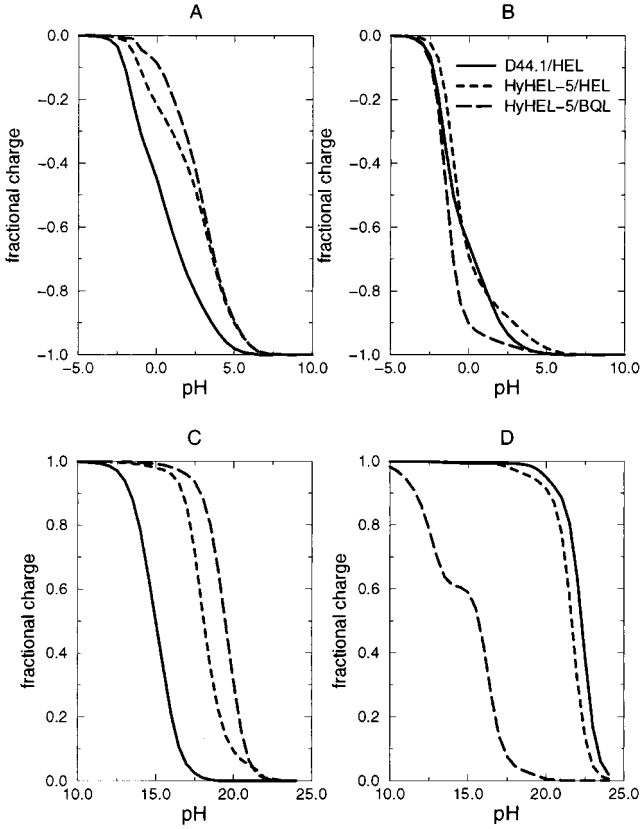

FIGURE 12: Titration curves of salt link residues in each of the three antibody-lysozyme complexes. (A) H Glu35; (B) H Glu50: (C) Y Arg45; (D) Y Arg68.

Table 3: Changes in Protonation Due to Complex Formation for Three Antibody/Lysozyme Pairs

	D44.1/HEL	HyHEL-5/HEL	HyHEL-5/BWQEL
		(A) pH = 7.0, $\epsilon = 20$	
H Glu35		−0.1	
H Glu50		−0.1	
		(B) pH = 7.0, $\epsilon = 4$	
L Glu42	0.2		
L Lys49	0.1		
H Glu10		−0.1	
H Glu35		0.3	0.3
H Glu50	−1.0	−1.0	−0.3
Y Trp1		0.1	
Y Lys33			−0.1
Y Glu35	−0.6	−0.8	
Y Asp48	−0.3	−0.1	
Y Asp2	−0.4	−0.7	−0.6
Y Asp66	−0.4	−1.0	0.8
Y Lys68			−1.0
Y Asp101	−0.1		
Y Lys116			−0.1

pH-Dependent Behavior of Constructed Mutants. The change in free energy due to complexation for each of the six constructed mutants to each antibody/protein complex is shown as a function of pH in Figure 13. In each case, the result of the mutation is as expected; binding is weakened by the mutation of the salt-link residues and largely unaffected by mutation of residues farther from the antibody/protein interface. Comparison of Figures 10 and 13B shows that the complexation energetics of hen egg lysozyme mutants R45K and R68K with HyHEL-5 are very similar to

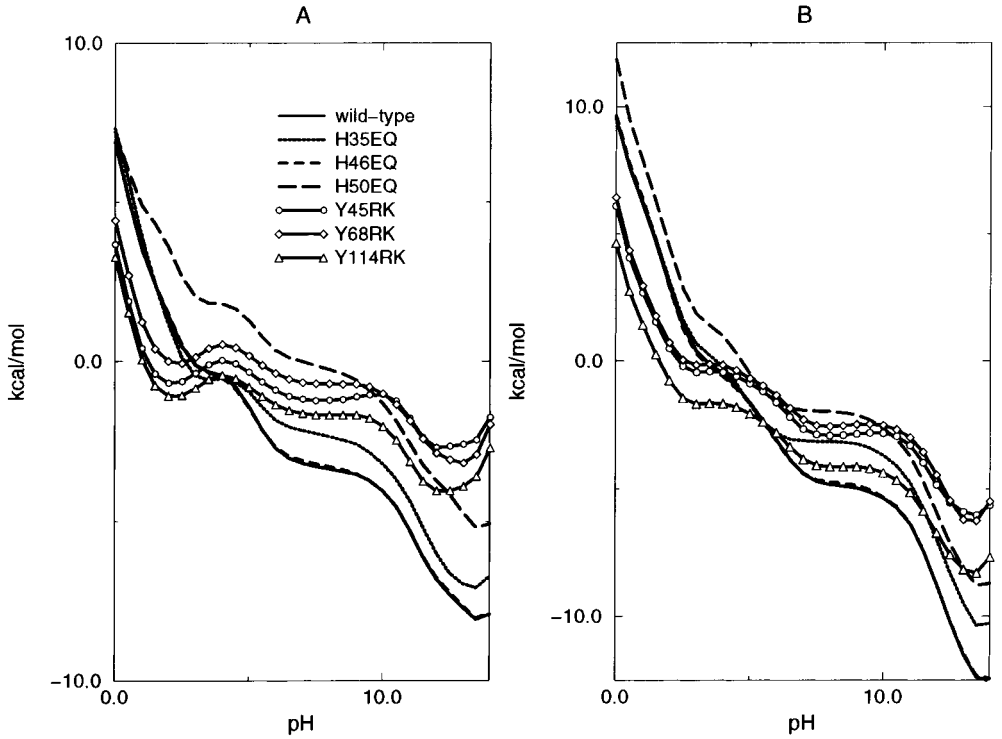

FIGURE 13: Change in free energy on binding (see Figure 10) for mutant antibody/lysozyme complexes, compared to wild type. (A) D44.1/HEL and mutants to the antibody or lysozyme. (B) HyHEL-5/HEL and mutants to the antibody or lysozyme.

Table 4: Residues for Which a Significant Change in pK_a Due to Binding Is Calculated, When Selected Water Molecules Are Included in the pK_a Calculation

	$\Delta[\Delta pK_a$(complex − free)](water − no water)		
residue[a]	D44.1/HEL	HyHEL-5/HEL	HyHEL-5/BWQEL
L His34/Tyr L 33	0.4	0.5	0.5
L Arg45		−0.3	−0.4
L Asp49		0.4	−0.4
L Tyr50	0.9		
L Arg96/92	0.3	0.0	0.0
H Glu35	0.1	−0.7	0.4
H Glu50	0.1	0.1	0.5
H Asp100	−0.2		
H Tyr103/101		0.2	0.1
Y Arg45	0.0	0.3	0.8
Y Tyr53			−0.7
Y Asp66	−0.2	0.0	−0.2
Y Arg68	0.1	0.4	0.5

[a] If two residue names or numbers are given, the first name or number refers to the residue in D44.1 and the second number refers to the corresponding residue in HyHEL-5.

Table 5: Differences in Change in Free Energy of Complex Formation Due to Various Mutations in the Antibody or in Lysozyme at pH 7.0

	$\Delta[\Delta G_{elec}$(complex − free)](mutant − wt)[a]	
mutation	D44.1/HEL	HyHEL-5/HEL
H E35 → Q	1.0	1.3
H E46 → Q	0.1	0.0
H E50 → Q	3.2	2.5
Y R 45 → K	2.0	1.8
Y R68 → K	2.4	2.1
Y R114 → K	1.6	0.6

[a] Values are given in kilocalories per mole.

the complexation energetics of BWQEL with HyHEL-5. It can be seen that similar values of ΔG_{elec} of complex formation are obtained over the entire pH range studied. D44.1 has also been shown experimentally to have less affinity for BWQEL than for HEL (Harper et al., 1987). While the pH dependence of ΔG_{elec} calculated for mutants to Arg45 and Arg68 in D44.1/HEL (Figure 13A) is somewhat different than the pH dependence calculated for HyHEL-5/BWQEL, it is more similar to the behavior of HyHEL-5/BWQEL than to either of the other wild-type complexes. The curve is somewhat flatter over the entire pH range, but the differences between mutant and wild type over most of the range are similar to the differences between the HyHEL-5 complexes with HEL and BWQEL. Differences in the free energy change on complexation due to mutations are summarized in Table 5. For modeled mutations of the salt-link-forming residues H 35, H 50, Y 45, and Y 68, differences in the electrostatic free energy change upon complex formation ranged between +1.0 and +3.2 kcal/mol. The differences in ΔG_{elec} of complex formation at pH 7.0, between the mutant-lysozyme HyHEL-5/HEL complexes and the wild type (1.8 and 2.1 kcal/mol, respectively), are very close to the calculated difference in ΔG_{elec} of complex formation between HyHEL-5/BWQEL and HyHEL-5/HEL (1.4 kcal/mol). The differences in interface surface area, the additional buried cavities present at the HyHEL-5/BWQEL interface, the different side chain rotamer state of K68 in the modeled mutant and in HyHEL-5/BWQEL, and the location of explicit solvent molecules used in the mutant models account for the difference in pH-dependent behavior between the HyHEL-5/BWQEL structure and the HyHEL-5/mutant HEL structure. These $\Delta\Delta G_{elec}$ values indicate that any of these mutations should decrease the affinity of the antibody for its antigen, though they do not take into account any possible structural rearrangements of the epitope or paratope regions due to the mutation, which may contribute to further changes in binding affinity. The differences in electrostatic free energy change upon complex formation fall within the normal range of free energy changes that have

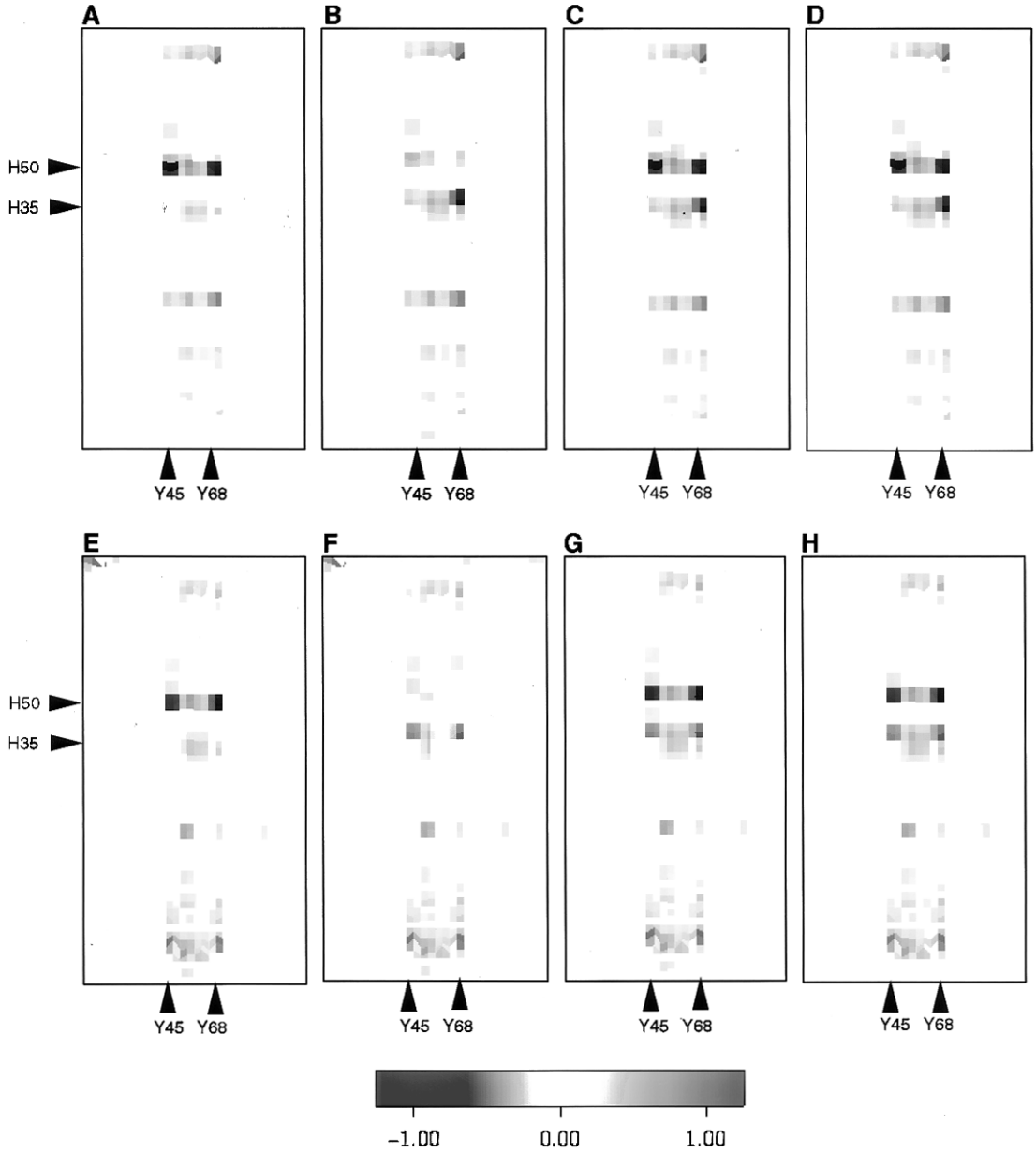

FIGURE 14: Electrostatic interaction maps. See caption to Figure 9. (Top) Interactions between residues in the lysozyme (*x*-axis) and antibody (*y*-axis) for mutants to the D44.1/HEL complex: (A) H E35 → Q, (B) H E50 → Q, (C) Y R45 → K, and (D) Y R68 → K. (Bottom) Interactions between residues in the lysozyme (*x*-axis) and antibody (*y*-axis) for mutants to the HyHEL-5/HEL complex: (E) H E35 → Q, (F) H E50 → Q, (G) Y R45 → K, (H) Y R68 → K.

been experimentally determined when salt bridges are introduced into or removed from proteins by mutagenesis, usually between 1 and 5 kcal/mol (Dao-Pin et al., 1991; Horovitz et al., 1990).

Shifts in pK_a due to the various mutations are localized to a very few residues near the site of the mutation. When mutations are made to any of the salt-link residues, the pK_a values calculated for the rest of the salt link, and for the same few nearby residues, shift; mutations to surface residues affect only residues in proximity to those mutations. The residues most affected by many of these mutations are those in the same cluster around the combining site, which have strong interactions with the salt-link residues: L Tyr33 in HyHEL-5 and its counterpart L His34 in D44.1; L Tyr35, L Arg96 in D44.1; H His98 and its replacement H Arg98 in D44.1; and H Tyr101 in HyHEL-5. Figure 14 shows the effect on site−site electrostatic interaction energies between the antibodies and HEL of mutations to the salt-link residues. Figures 15 and 16 show shifts in pK_a vs sequence number due to mutations in the D44.1/HEL and HyHEL-5/HEL complexes, respectively. Electrostatic energy changes and pK_a shifts are for the most part localized to those residues in immediate contact with the mutated residue, with the remainder of the interaction map changing little if at all. The interaction between H Glu35 and H Glu50 causes a pK_a shift to one of these residues if the other is replaced by Gln even in the free antibody, while the mutations to either one of the Arg residues in the free lysozyme have little or no effect on the titration equilibrium of the other. This is to some extent due to the two Glu residues being buried in a cleft in the antibody and interacting with each other within the low-dielectric region, while the two Arg residues protrude into the high-dielectric region from the surface of the lysozyme molecule and are thus better screened from each other. In both the D44.1 and HyHEL-5 complexes with HEL and BWQEL, the titration of the residue H Glu35 is most strongly

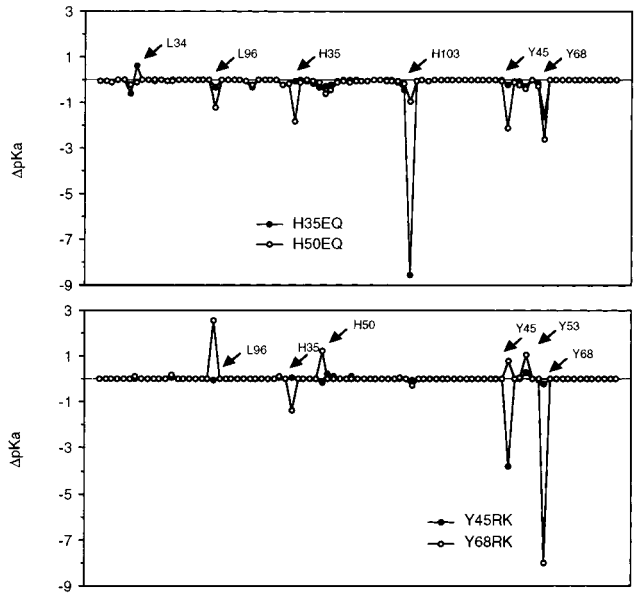

FIGURE 15: pK_a shifts due to various mutations, vs titrating site number, for the D44.1/HEL complex. The traces are separated into mutants to the antibody, in the top plot, and mutants to the lysozyme, in the bottom plot, for clarity.

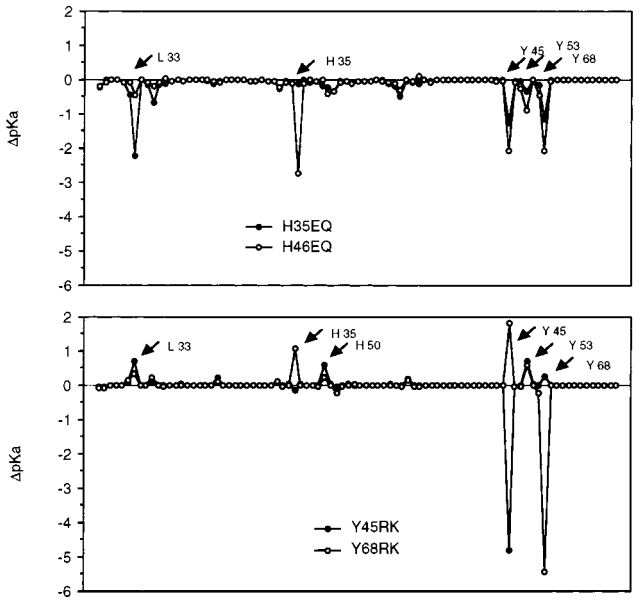

FIGURE 16: pK_a shifts due to various mutations, vs titrating site number, for the HyHEL-5/HEL complex. The traces are separated into mutants to the antibody, in the top plot, and mutants to the lysozyme, in the bottom plot, for clarity.

affected by the mutation of H Glu50 and Y Arg68 of the lysozyme, while the residue H Glu50 is affected by removal of H 35 but is more strongly affected by the change of Y Arg68 to Lys in D44.1, and by Y Arg45 → Lys in HyHEL-5. Y Arg68 is affected significantly only by the alteration of H Glu35 and H Glu50, while Y Arg45 is also affected by the alteration of Y 68 and is not affected by the alteration of H 35, in D44.1. In no case, however, does a mutation change the charge state of any of the salt-link residues at pH 7.0, as shown in Table 6.

Table 6: Predicted Fractional Charge on Salt Link Residues in the Antibody/Lysozyme Complexes at pH 7.0

protein	H35	H50	Y45	Y68
		D44.1/HEL		
WT	−1.0	−1.0	1.0	1.0
H E 35 → Q		−1.0	1.0	1.0
H E50 → Q	−1.0		1.0	1.0
Y R45 → K	−1.0	−1.0	1.0	1.0
Y R68 → K	−1.0	−1.0	1.0	1.0
		HyHEL-5/HEL		
WT	−1.0	−1.0	1.0	1.0
H E35 → Q		−1.0	1.0	1.0
H E50 → Q	−1.0		1.0	1.0
Y R45 → K	−1.0	−1.0	1.0	1.0
Y R68 → K	−1.0	−1.0	1.0	1.0

DISCUSSION

The affinity of antibodies for their protein ligands is controlled by a number of factors, which are difficult to delineate. The presence of salt links at the protein interface is important for binding, and the loss of one of these interactions in the HyHEL-5/BWQEL complex, due to the substitution of Lys for Arg at position 68, does reduce affinity substantially compared to HyHEL-5/HEL. However, the affinity of HyHEL-5 for BWQEL is still greater than that of D44.1 for HEL, despite the fact that three salt links exist in the D44.1/HEL complex. When the charged residues in the antibody combining site, H Glu35 or H Glu50, are replaced by neutral polar residues, there is a resulting loss of a favorable charge−charge interaction on the order of −1 to 1.5 kcal/mol (Figure 14). No significant new interactions compensate for this loss. This results in reduced calculated affinity of the mutant antibody for lysozyme. Site-directed mutagenesis experiments in which the salt-link residues are replaced with nonpolar residues, either singly or in pairs, will be required to determine the actual contribution of these salt links to the complexation energetics. Replacement of a charge−charge interaction with a hydrophobic contact may be energetically favorable (Hendsch & Tidor, 1994); while salt links have been found in some antibody/antigen interactions, other protein complexes form without significant charge−charge interaction (Janin, 1995).

In all three of the native antibody/lysozyme complexes studied, the change in free energy on antibody binding to the antigen was found to be strongly dependent on pH. ΔG_{elec} of complex formation is a relatively constant, negative value, above pH 5.0 and below pH 10.0. The magnitude of ΔG_{elec} begins to decrease at about pH 5.0, as the glutamic acid residues in the antibody combining region become protonated. There are two effects that cooperate to make binding unfavorable at low pH: the loss of the energetically favorable salt-link interactions between the charged glutamic acid and arginine residues and the energy penalty for burying the arginine charges in the largely nonpolar interface. Below approximately pH 2.5, ΔG_{elec} of complex formation is positive. At high pH, the Arg residues in the combining region become deprotonated and ΔG_{elec} becomes large and negative as the energy penalty for burying these charges at the interface is removed. While the favorable salt-link interactions are lost at high pH, there is little added energy penalty for burying the glutamic acid charges at the interface; these residues are mostly inaccessible to solvent in the free antibody structure.

The substitution of Lys for Arg68 in BWQEL is a conservative mutation that should result in little change in affinity if specific interactions between ionized residues were the sole determinant of affinity. However, it is clear that the electrostatics of this ionic interaction is modulated by

the different solvation environment created by the Arg → Lys mutation. We note here that one difference between the HyHEL-5/BWQEL interface and the HyHEL-5/HEL interface is that there are a larger number of water molecules present in HyHEL-5/BWQEL. Cavities at this interface are larger than in the other complex, resulting in an interface that is arguably less rigidly structured, as well as more solvated, than the interface in HyHEL-5/HEL. This results in a higher effective dielectric constant at the antibody/protein interface in HyHEL-5/BWQEL, which reduces the magnitude of electrostatic interactions.

There are subtle differences in the antibody combining geometry that result in different salt link configurations in D44.1/HEL and HyHEL-5/HEL. The geometry of the HyHEL-5/HEL complex results in larger cavities near the interface and larger numbers of bound solvent-inaccessible water molecules than are found in D44.1. The interaction between H Glu35 and Y Arg68 in HyHEL-5 is mediated by a water molecule in the HyHEL-5/HEL structure, whereas it is a direct interaction in the D44.1/HEL structure. On this basis alone it might be expected that D44.1 would have a greater affinity for HEL than HyHEL-5. However, H Glu35 in D44.1 also participates in an intramolecular interaction with L Arg96 (Figure 4), and the bifurcated interaction results in a weaker link to Y Arg68 by D44.1. These differences in salt-link geometry result not only from isolated residue replacements in the CDR regions, such as the replacement of Ser with Tyr at position L 94 in D44.1, but also from differences in the antibody framework as a whole. By mutation of salt-link residues in either the D44.1/HEL complex or the HyHEL-5/HEL complex, we change the pH dependence and magnitude of ΔG_{elec} of complex formation. Mutation of the arginine side chains participating in these salt links, in the HyHEL-5/HEL complex, results in pH-dependent behavior similar to that of the HyHEL-5/BWQEL complex. Calculated $\Delta\Delta G_{elec}$ values for R45K and R68K mutants D44.1/HEL complexes suggest that such mutants would have a reduction in affinity similar to that of HyHEL-5/BWQEL relative to HyHEL-5/HEL. Loop-swapping experiments in which CDR loops from D44.1 are grafted to the framework of HyHEL-5 and vice versa may help elucidate the reasons for differences in combining geometry and resulting differences in affinity. However, at least for the V_H region, both antibodies possess the same type of framework out of three different frameworks that have been described (Saul & Poljak, 1993). There are a number of other ways in which the sequence of HyHEL-5 might be systematically mutated toward the sequence of D44.1, or vice versa, to understand the subtle structural determinants of affinity. Entire replacement of the L or H chain of one antibody with that of the other, replacement of selected framework and CDR regions, or even systematic single-residue replacement are possible approaches, though it is unlikely that a single change or even modification of a whole loop or strand will be the switch that converts a HyHEL-5/HEL-like complex into a D44.1/HEL-like complex.

An important difference that contributes to the greater affinity of HyHEL-5 for HEL is the amount of surface area buried in each of the complexes. An area of 1248 Å^2 is buried at the interface of D44.1 and HEL (Braden et al., 1994), while 1510 Å^2 is buried at the interface of HyHEL-5 and HEL (Davies & Cohen, 1996). Van der Waals interactions are thought to be ultimately more significant in protein−protein interactions than are hydrogen bonds or salt links (Ross & Subramanian, 1981; Janin, 1995). The combining site of HyHEL-5 and HEL can be seen to be surrounded by an annulus of hydrophobic residues, which form contacts that shield the polar residues in the combining site from bulk solvent; this is not true at the interface of D44.1 and HEL. This insulation by nonpolar residues has implications both for van der Waals interactions and for electrostatic interactions at the antibody/lysozyme interface, in that it alters the effective dielectric constant in the interface. Engineering such an annulus of hydrophobic residues around the combining site of D44.1 and/or reducing the hydrophobic buried area in HyHEL-5/HEL is an ideal test of the significance of hydrophobic interactions and hydrophobic shielding of polar interactions for protein association energetics.

ACKNOWLEDGMENT

We thank Dr. Jie Liang for assistance in the use of VOLBL, to compute molecular surface areas; and Dr. Barry Honig for providing the program GRASP, for the display of electrostatic potentials.

REFERENCES

Alegre, M. L., Collins, A. M., Pulito, V. L., Brosius, R. A., Olson, W. C., Zivin, R.A., Knowles, R., Thistlethwaite, J. R., Jolliffe, L. K., & Bluestone, J. A. (1992) *J. Immunol. 148*, 3461.

Amit, A. G., Mariuzza, R. A., Phillips, S. E. V., & Poljak, R. J. (1986) *Science 233*, 747−753.

Antosiewicz, J., McCammon, J. A., & Gilson, M. K. (1994) *J. Mol. Biol. 238*, 415−436.

Ban, N., Escobar, C., & Garcia, R. (1994) *Proc. Natl. Acad. Sci. U.S.A. 91*, 1604.

Benjamin, D. C., Williams, D. C., Jr., Smith-Gill, S. J., & Rule, G. S. (1992) *Biochemistry 31*, 9539−9545.

Bentley, G. A., Boulot, G., Riottot, M. M., & Poljak, R. J. (1990) Nature 348, 254.

Bhat, T. N., Bentley, G. A., Fischmann, T. O., Boulot, G., & Poljak, R. J. (1990) *Nature (London) 347*, 483.

Bhat, T. N., Bentley, G. A., Boulot, G., Greene, M. I., Tello, D., Dall'acqua, W., Souchon, H., Schwartz, F. P., & Mariuzza, R. A. (1994) *Proc. Natl. Acad. Sci. U.S.A. 91*, 1089.

Bizebard, T., Gigant, B., Rigolet, P., Rasmussen, B., Diat, O., Bosecke, P., Wharton, S. A., Skehel, J. J., & Knossow, M. (1995) *Nature 376*, 92.

Bossart-Whitaker, P., Chang, C. Y., Novotny, J., Benjamin, D. C., & Sheriff, S. (1995) *J. Mol. Biol. 253*, 559.

Braden, B. C., & Poljak, R. J. (1995) *FASEB J. 9*, 9.

Braden, B. C., Souchon, H., Eisele, J.-L., Bentley, G. A., Bhat, T. N., Navaza, J., & Poljak, R. J. (1994) *J. Mol. Biol. 243*, 767.

Braden, B. C., Fields, B. A., & Poljak, R. J. (1995) *J. Mol. Recog. 8*, 317.

Braden, B. C., Fields, B. A., Ysern, X., Goldbaum, F. A., Dall'acqua, W., Schwarz, F. P., Poljak, R. J., & Mariuzza, R. A. (1996) *J. Mol. Biol. 257*, 889.

Brooks, B. R., Bruccoleri, R. E., Olafson, B. D., States, D. J., Swaminathan, S., & Karplus, M. (1982) *J. Comput. Chem. 4*, 187.

Brunger, A. T., & Karplus, M. (1988) *Proteins: Struct., Funct., Genet. 4*, 148.

Buckle, A. M., Schreiber, G., & Fersht, A. R. (1994) *Biochemistry 33*, 8878.

Chacko, S., Silverton, E., Kam-Morgan, L., Smith-Gill, S., Cohen, G., & Davies, D. (1995) *J. Mol. Biol. 245*, 261.

Chacko, S., Silverton, E. W., Smith-Gill, S., Davies, D. R., Shick, K. A., Xavier, K. A., Willson, R. C., Jeffrey, P. D., Chang, C. Y. Y., Sieker, L. C., & Sheriff, S. (1996) *Proteins: Struct., Funct., Genet. 26*, 55.

Chitarra, V., Alzari, P. M., & Bentley, G. A. (1993) *Proc. Natl. Acad. Sci. U.S.A. 90*, 7711.

Cohen, G. H., Sherriff, S., & Davies, D. R. (1996) *Acta Crystallogr. 52*, 315.
Dao-Pin, S., Sauer, U., Nicholson, H., & Matthews, B. W. (1991) *Biochemistry 30*, 7142.
Davies, D. R., & Cohen, G. H. (1996) *Proc. Natl. Acad. Sci. U.S.A. 93*, 7.
Davis, M. E., Madura, J. D., Luty, B. A., & McCammon, J. A. (1991) *Comput. Phys. Commun. 62*, 187.
Edelsbrunner, H., Facello, M., Fu, P., & Liang, J. (1995) in *Proceedings of the 28th Annual Hawaii International Conference on System Sciences*, p 256, IEEE Computer Society Press, Los Alamitos, CA.
Fields, B. A., Goldbaum, F. A., Ysern, X., Poljak, R. J., & Mariuzza, R. A. (1995) *Nature 374*, 739.
Fischmann, T. O., Bentley, G. A., Bhat, T. N., Boulot, G., Mariuzza, R. A., Phillips, S. E. V., Tello, D., & Poljak, R. J. (1991) *J. Biol. Chem. 266*, 12915.
Gibas, C. J., & Subramaniam, S. (1996) *Biophys. J. 71*, 138.
Gilson, M. K. (1993) *Proteins: Struct., Funct., Genet. 15*, 266.
Goldbaum, F. A., Schwarz, F. P., Eisenstein, E., Cauerhff, A., Mariuzza, R. A., & Poljak, R. J. (1996) *J. Mol. Recog. 9*, *6*.
Harper, M., Lema, F., Boulot, G., & Poljak, R. J. (1987) *Mol. Immunol. 2*, 97.
Hendsch, Z. S., & Tidor, B. (1994) *Protein Sci. 3*, 211.
Hibbits, K. A., Gill, D. S., & Willson, R. C. (1994) *Biochemistry 33*, 3584.
Horovitz, A., Serrano, L., Avron, B., Bycroft, M., & Fersht, A. R. (1990) *J. Mol. Biol 216*, 1031.
Janin, J. (1995) *Biochimie 77*, 497.
Jorgensen, W. L., & Tirado-Rives, J. (1988) *J. Am. Chem. Soc 110*, 1657.
Knossow, M., Daniels, R. S., Douglas, A. R., Skehel, J. J., & Wiley, D. C. (1984) *Nature (London) 311*, 678.
Lavoie, T. B., Kam-Morgan, L. N. W., Mallet, C. P., Schilling, J. W., Prager, E. M., Wilson, A. C., & Smith-Gill, S. J. (1990) in *Use of X-ray Crystallography in the Design of Antiviral Agents* (Laver, W. G., & Air, G. M., Eds.), Academic Press, New York.
Lescar, J., Pellegrini, M., Souchon, H., Tello, D., Poljak, R. J., Peterson, N., Greene, M., & Alzari, P. M. (1995) *J. Biol. Chem. 270*, 18067.
Liang, J., Sudhakar, P. V., Edelsbrunner, H., Fu, P., & Subramaniam, S. (1997) *Proteins: Struct., Funct., Genet.* (in press).
Madura, J. D., Briggs, J. M., Wade, R. C., Davis, M. E., Luty, B. A., Ilin, A., Antosiewicz, J., Gilson, M. K., Bagheri, B., Scott, L. R., & McCammon, J. A. (1995) *Comput. Phys. Commun. 91*, 57.
McDonald, I. K., & Thornton, J. M. (1994) *J. Mol. Biol. 238*, 777.
McDonald, S. M., Willson, R. C., & McCammon, J. A. (1995) *Protein Eng. 8*, 915.
Nicholls, A., Sharp, K., & Honig, B. (1991) *Proteins: Struct., Funct., Genet. 11*, 281.
Padlan, E. A., Silverton, E. W., Sheriff, S., Cohen, G. H., Smith-Gill, S. J., & Davies, D. R. (1989) *Proc. Natl. Acad. Sci. U.S.A. 86*, 5938.
Prasad, L., Sharma, S., Vandonselaar, M., Quail, J. W., Lee, J. S., Waygood, E. B., Wilson, K. S., Dauter, Z., & Delbaere, L. T. J. (1993) *J. Biol. Chem. 268*, 10705.
Ross, P. D., & Subramanian, S. (1981) *Biochemistry 20*, 3096.
Saul, F. A., & Poljak, R. J. (1993) *J. Mol. Biol. 230*, 15.
Schwarz, F. P., Tello, D., Goldbaum, F. A., Mariuzza, R. A., & Poljak, R. J. (1995) *Eur. J. Biochem. 228*, 388.
Sheriff, S., Silverton, E. W., Padlan, E. A., Cohen, G. H., Smith-Gill, S. J., & Davies, D. R. (1987) *Proc. Natl. Acad. Sci. U.S.A. 84*, 8075.
Shrake, A., & Rupley, J. A. (1973) *J. Mol. Biol. 79*, 351.
Smith-Gill, S. J., Wilson, A. C., Potter, M., Prager, E. M., Feldmann, R. J., & Mainhart, C. R. (1982) *J. Immunol. 28*, 314.
Tanford, C., & Roxby, R. (1972) *Biochemistry 11*, 2192.
Tello, D., Goldbaum, F. A., Mariuzza, R. A., Ysern, X., Schwarz, F. P., & Poljak, R. J. (1993) *Biochem. Soc. Trans. 21*, 943.
Tulip, W. R., Varghese, J. N., Laver, W. G, Webster, R. G., & Colman, P. M. (1992a) *J. Mol. Biol. 227*, 122.
Tulip, W. R., Varghese, J. N., Webster, R. G., Laver, W. G, & Colman, P. M. (1992b) *J. Mol. Biol. 227*, 149.
Wallace, A. C., Laskowski, R. A., & Thornton, J. M. (1995) *Protein Eng. 8*, 127.

BI9701989